Supporting Information

Nagai et al. 10.1073/pnas.1115749108

SI Methods.

Materials. We synthesized 3-methylene-4-penten-1-yl diphosphate (vIPP) and 3-oxiranyl-3-buten-1-yl diphosphate (oIPP) as described previously (1, 2). [1-^{14}C]IPP was purchased from American Radiolabeled Chemicals, Inc. All other chemicals were of analytical grade.

Enzyme Purification. Polyhistidine-tagged *Sulfolobus shibatae* type-2 isopentenyl diphosphate isomerase (IDI-2) was expressed in *Escherichia coli* BL21(DE3)/pET-idi (3). The transformant was cultivated in LB medium containing 50 mg/L ampicillin until cells reached the early stationary phase. The recombinant enzyme was extracted from harvested cells and purified by heat treatment at 55 °C for 30 min and a HisTrap column (GE Healthcare) as described previously (4). For crystallization experiments, the polyhistidine tag was then removed with Thrombin Restriction Grade (Novagen), and the enzyme was recovered in the flow-through fraction from a second HisTrap column. The buffer was exchanged by dialysis to Buffer A, containing 10 mM Tris·HCl, pH 7.7, 1 mM EDTA, and 10 mM 2-mercaptoethanol. The dialyzed enzyme solution was loaded on a Mono Q 5/50 column (GE Healthcare) and eluted with a linear gradient of 0–0.3 M NaCl in Buffer A. The active fractions were combined and then concentrated by centrifugation with Amicon Ultra 10K centrifugal filters (MILLIPORE). The enzyme was chromatographed on a HiLoad 16/60 Superdex 200 column (GE Healthcare) upon elution with Buffer A containing 0.15 M NaCl.

Polyhistidine-tagged *Thermus thermophilus* IDI-2 was expressed in *E. coli* and purified as previously described (5, 6) or slightly modified as follows. Cells were grown in Terrific broth containing 200 mg/L riboflavin, 100 μg/mL ampicillin, and 34 μg/mL chloramphenicol at 37 °C. After 4 h, 0.4 mM IPTG was added and after an additional 4 h, the cultures were harvested and yielded 4.3 g of cell paste per liter of media. The purification steps were modified by using a HisTrap high-performance column (GE Healthcare) with a flow rate of approximately 5 mL/ min and eluting with 50 mM Na_2HPO_4, 500 mM imidazole, and 300 mM NaCl, pH 8.

Crystallization. Crystals of *S. shibatae* IDI-2 were grown at 20 °C using the sitting-drop vapor-diffusion method with a reservoir solution containing 0.1 M Tris·HCl, pH 8.0, 0.2 M sodium citrate, and 30% (vol/vol) polyethylene glycol 400 (PEG400). To obtain IDI-2-oIPP, crystals of IDI-2 were soaked for 3 h in a reservoir solution containing 32% (vol/vol) PEG400, 12.5 mM $MgCl_2$, 20 mM NADH, and 4 mM oIPP. For vIPP-IDI structure, 4 mM vIPP was used instead of oIPP, and soaking was performed for 1 h. To obtain IDI-2·IPP and IDI-2·dimethylallyl diphosphate (DMAPP), crystals were soaked for 1 h in the reservoir solution containing 35% (vol/vol) PEG400, 12.5 mM $MgCl_2$, and 5 mM IPP or 10 mM DMAPP, respectively, and then $Na_2S_2O_4$ (20 mM final concentration) was added to the soaking solution to reduce the crystals for 10 min. Crystals were immediately mounted in the X-ray diffraction apparatus.

Data Collection, Structure Solution, and Refinement. All datasets were collected on beamlines BL-5A and NE-3A at the photon factory (KEK, Tsukuba, Japan). X-ray diffraction data of crystals were processed and scaled with HKL2000 (7). Data collection statistics are summarized in Table 1. IDI structures were refined using the program Refmac (8) from the CCP4 suite and atomic coordinate of $FreeIDI_{red}$ (Protein Data Bank code 2ZRV). Manual fitting of the model was carried out using the program Coot (9). vIPP- and oIPP-adduct, IPP, and DMAPP models were fitted into the substrate-binding sites based on the difference electron density map. The refinement statistics are summarized in Table 1. The figures for the protein models were drawn using the programs PyMOL (10) and Coot (Fig. 1*D*).

Mass Spectrometry. Inhibited *S. shibatae* IDI-2 was denatured as described above and the protein was removed by filtration. The flavin-inhibitor adducts were mixed with an equal volume of acetonitrile containing 1% (vol/vol) triethylamine and analyzed by negative-ion electrospray ionization-mass spectrometry with an Esquire 3000 (BRUKER) by direct infusion.

Mutagenesis. Site-directed mutations on *S. shibatae* IDI-2 were introduced into pET-idi using a QuikChange Mutagenesis Kit (STRATAGENE) and oligonucleotide primers indicated in Table S2.

Mutant Enzyme Assay. Assays for *S. shibatae* IDI-2 were conducted as described in our previous paper (11), excepting that 0.5–1 μM [1-^{14}C]IPP (2 GBq/mmol) and an appropriate amount of the purified enzyme were used.

1. Walker JR, Rothman SC, Poulter CD (2008) Synthesis and evaluation of substrate analogues as mechanism-based inhibitors of type II isopentenyl diphosphate isomerase. *J Org Chem* 73:726–729.
2. Wu Z, Wouters J, Poulter CD (2005) Isopentenyl diphosphate isomerase. Mechanism-based inhibition by diene analogues of isopentenyl diphosphate and dimethylallyl diphosphate. *J Am Chem Soc* 127:17433–17438.
3. Yamashita S, Hemmi H, Ikeda Y, Nakayama T, Nishino T (2004) Type 2 isopentenyl diphosphate isomerase from a thermoacidophilic archaeon *Sulfolobus shibatae*. *Eur J Biochem* 271:1087–1093.
4. Unno H, et al. (2009) New role of flavin as a general acid-base catalyst with no redox function in type 2 isopentenyl-diphosphate isomerase. *J Biol Chem* 284:9160–9167.
5. de Ruyck J, Rothman SC, Poulter CD, Wouters J (2005) Structure of *Thermus thermophilus* type 2 isopentenyl diphosphate isomerase inferred from crystallography and molecular dynamics. *Biochem Biophys Res Commun* 338:1515–1518.
6. Rothman SC, Helm TR, Poulter CD (2007) Kinetic and spectroscopic characterization of type II isopentenyl diphosphate isomerase from *Thermus thermophilus*: Evidence for formation of substrate-induced flavin species. *Biochemistry* 46:5437–5445.
7. Otwinowski Z, Minor W (1997) Processing of X-ray diffraction data collected in oscillation mode. *Methods Enzymol* 276:307–326.
8. Murshudov GN, Vagin AA, Dodson EJ (1997) Refinement of macromolecular structures by the maximum-likelihood method. *Acta Crystallogr D Biol Crystallogr* 53:240–255.
9. Emsley P, Cowtan K (2004) Coot: Model-building tools for molecular graphics. *Acta Crystallogr D Biol Crystallogr* 60:2126–2132.
10. DeLano WL (2002) The PyMOL molecular graphics system (Schrödinger, Portland, OR).
11. Hemmi H, Ikeda Y, Yamashita S, Nakayama T, Nishino T (2004) Catalytic mechanism of type 2 isopentenyl diphosphate:dimethylallyl diphosphate isomerase: Verification of a redox role of the flavin cofactor in a reaction with no net redox change. *Biochem Biophys Res Commun* 322:905–910.

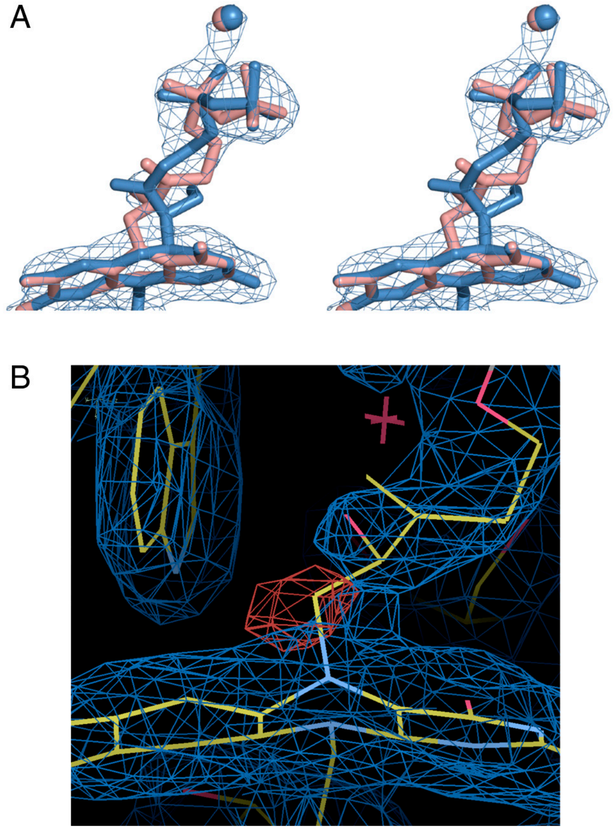

Fig. S1. Structural information of the flavin adducts formed in *S. shibatae* IDI-2 by treatment with oIPP. (*A*) C4a and N5 adduct model structures for oIPP-IDI with density map. The C4a and N5 models are shown in blue and pink, respectively. Mg^{2+} ions are indicated in spheres. The electron map (blue) is contoured at 1.3σ. The C4a and N5 models were constructed with the most likely chemical structures of oIPP adduct—i.e., **10** and **15** in Fig. S2, respectively. (*B*) $2F_o - F_c$ and noncrystallography symmetry-averaged $F_o - F_c$ maps overlapping the N5-model structure of oIPP-IDI. The electron maps of $2F_o - F_c$ (blue) and $F_o - F_c$ (red) are contoured at 1.3σ and −4.0σ, respectively. Carbon, oxygen, and nitrogen atoms are colored yellow, red, and blue, respectively.

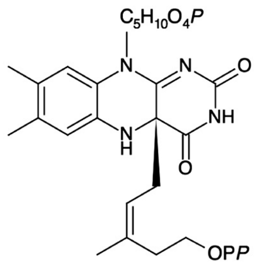

1

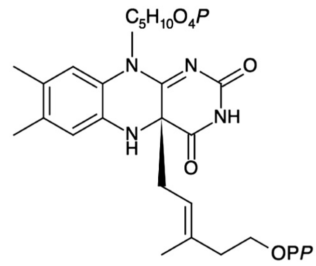

2

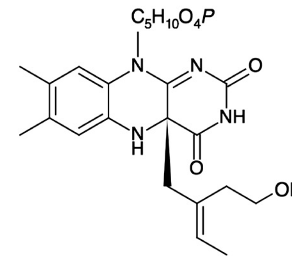

3

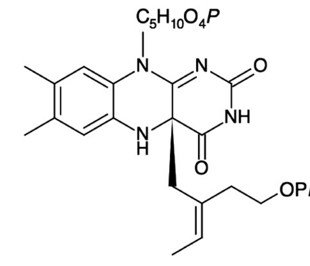

4

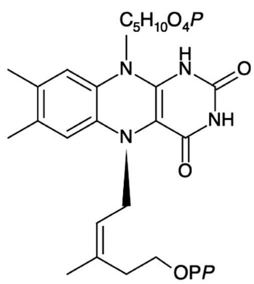

5

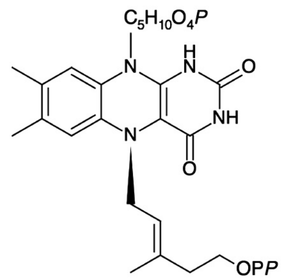

6

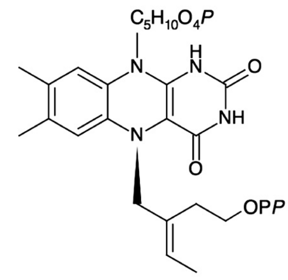

7

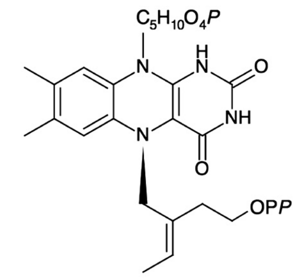

8

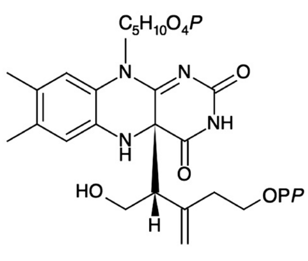

9

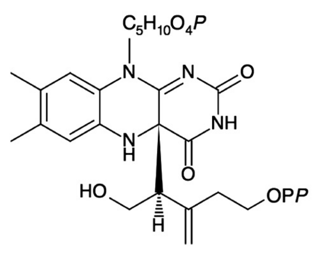

10

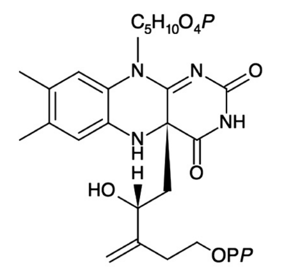

11

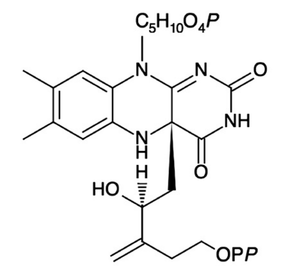

12

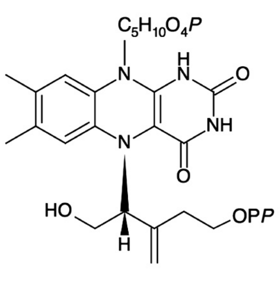

13

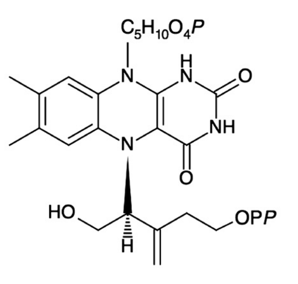

14

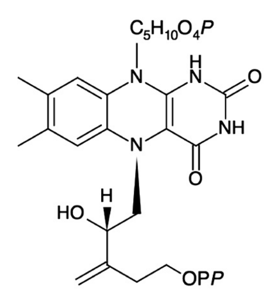

15

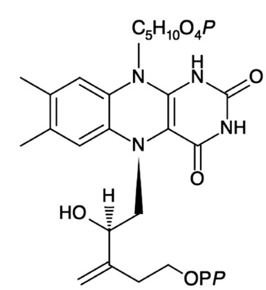

16

Fig. S2. Possible chemical structures of vIPP and oIPP adducts. The isomer numbering is the same with that used in Table S1. $C_5H_{10}O_4P$ and OPP mean ribitol phosphate and diphosphate groups, respectively. Isomers **3**, **4**, and **5** are the chemical structures of vIPP adduct used for the construction of the C4a and N5 models in Fig. 1, respectively.

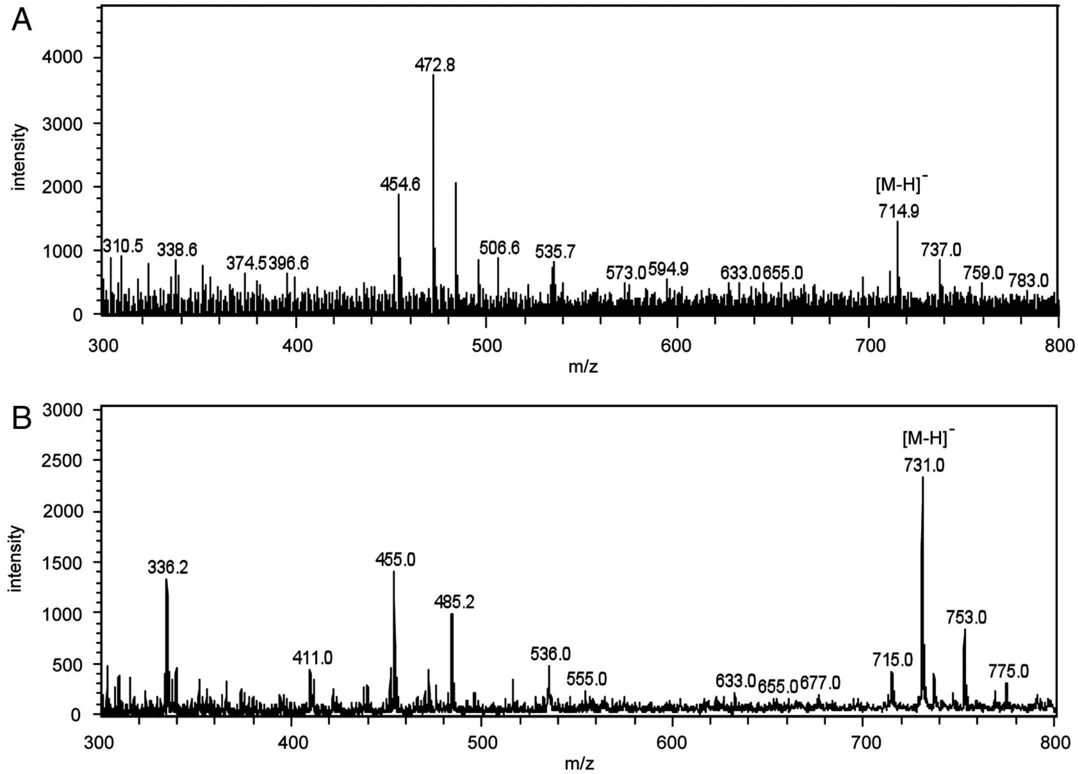

Fig. S3. Electrospray ionization mass spectra of flavin adducts from *S. shibatae* IDI-2. (*A*) vIPP-FMN_{red}. (*B*) oIPP-FMN_{red}.

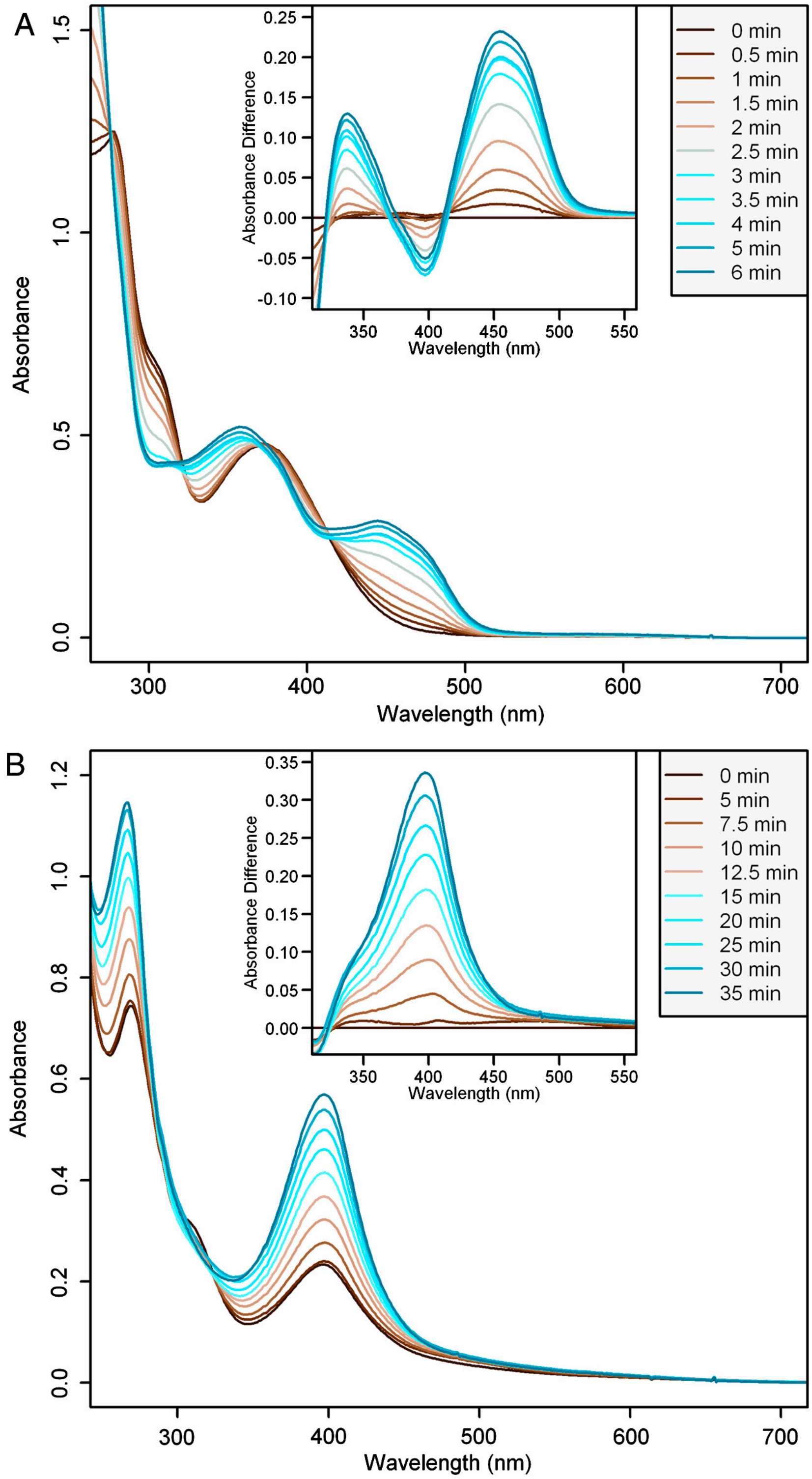

Fig. S4. Spectral changes through the photooxidation of vIPP adduct from *T. thermophilus* IDI-2. Time-dependent change in UV-visible spectra of free vIPP adduct upon photooxidation at pH 6 with an inset of the difference spectrum of the traces between $t = 0$ and $t = 6$ min (*A*) and in 6N HCl with an insert of the difference spectra between $t = 0$ and $t = 35$ min (*B*).

Table S1. Map correlation coefficients of the vIPP and oIPP adducts with different isomeric structures

	Map correlation coefficient*			
		Hydrocarbon (inhibitor)		
Isomers[†]	Overall	FMN		Diphosphate
vIPP adduct				
vIPP adduct				
1	0.9312	0.9341	0.9242	0.9262
2	0.9279	0.9346	0.9046	0.9122
3	0.9307	0.9348	0.9435	0.9187
4	0.9319	0.9375	0.9327	0.9184
5	0.9290	0.9345	0.9414	0.9113
6	0.9329	0.9378	0.9013	0.9277
7	0.9306	0.9349	0.9076	0.9290
8	0.9326	0.9364	0.9171	0.9289
oIPP adduct				
9	0.9159	0.9369	0.8828	0.8699
10	0.9143	0.9374	0.8867	0.8645
11	0.9131	0.9359	0.8596	0.8607
12	0.9139	0.9359	0.8776	0.8615
13	0.9159	0.9385	0.8550	0.8677
14	0.9148	0.9369	0.8745	0.8639
15	0.9148	0.9366	0.8848	0.8628
16	0.9147	0.9388	0.8606	0.8612

*Map correlation coefficients were calculated using the OVERLAPMAP program in the CCP4 suite 1. Among the coefficients separately calculated for FMN, inhibitor-derived hydrocarbon, and diphosphate units in the overall adduct structures, those for the hydrocarbon unit (including epoxy-derived oxygen in the case of oIPP adduct) are more variable and were used to determine which isomer is the most likely.

[†]The isomer numbering is the same as that used in Fig. S2. Isomers **3**, **4**, and **5** are the chemical structures of vIPP adduct used for the construction of the C4a and N5 models in Fig. 1, respectively. Isomers **10** and **15** are the chemical structures of oIPP adduct used for the construction of the C4a and N5 models in Fig. S1, respectively.

1 Collaborative Computational Project Number 4 (1994) The CCP4 suite: Programs for protein crystallography. *Acta Crystallogr D Biol Crystallogr* 50:760–763.

Table S2. Oligonucleotide primers used for mutagenesis

Mutant	Primer sequence*
Q160E	CTTAAATCCGGCAGAGGAAGTATTTCAAC
Q160H	CTTAAATCCGGCCCATGAAGTATTTCAAC
Q160K	CTTAAATCCGGCCAAAGAAGTATTTCAAC
Q160L	CTTAAATCCGGCCCTAGAAGTATTTCAAC
Q160N	CTTAAATCCGGCCAATGAAGTATTTCAAC

*For mutagenesis, the primers indicated and primers with complementary sequences were used.